

# Synthesis of Chitosan-*ortho*-vanillin/AgNPs Schiff Base Composite as Food Preservative

Ismiyarto Ismiyarto<sup>1\*</sup>, Istikmaala Rosyadi Putri<sup>1</sup>, Dwi Susilo<sup>1,2</sup>, Purbowatiningrum Ria Sarjono<sup>1</sup>, Ngadiwiyanana Ngadiwiyanana<sup>1</sup>, Muhammad Cholid Djunaidi<sup>1</sup>, Damar Nurwahyu Bima<sup>1</sup>, Gan B. Bajracharya<sup>3</sup>, Marcelinus Christwardana<sup>1</sup>

<sup>1</sup> Department of Chemistry, Faculty of Science and Mathematics, Diponegoro University, Jl. Prof. H. Soedarto, 50275 Semarang, Indonesia

<sup>2</sup> National Environmental Public Health Laboratory, Ministry of Health Indonesia, Hasanudin Street 123., 50721 Salatiga, Indonesia

<sup>3</sup> Laboratory of Catalysis and Frontier Molecules, Faculty of Science, Nepal Academy of Science and Technology (NAST), Khumaltar, Lalitpur, Nepal

\* Corresponding author, e-mail: [ismiyarto@live.undip.ac.id](mailto:ismiyarto@live.undip.ac.id)

Received: 17 October 2024, Accepted: 29 January 2025, Published online: 28 February 2025

## Abstract

Structural modification of chitosan (CH) may enhance the stability of silver nanoparticles (AgNPs) synthesized. This study aims to modify chitosan into chitosan-*ortho*-vanillin Schiff base (CHoVSB), which was used as a capping agent in the synthesis of AgNPs, and were evaluated as the food preservative through the antimicrobial testing. Composites of AgNPs were synthesized using AgNO<sub>3</sub> as an Ag precursor, ascorbic acid as a bioreductor, sodium tripolyphosphate (STTP) as a crosslinker and chitosan or CHoVSB. They were characterized by ultraviolet-visible (UV-Vis), Fourier transform infrared spectroscopy (FTIR), atomic absorption (AA) and scanning electron microscope-energy dispersive X-ray (SEM-EDX) analyses. CHoVSB was synthesized as a brownish-yellow solid with a yield of 57.6% and a degree of substitution of 44.09%. The composites of CH/AgNP were brownish-yellow solids with yields of 80.8–83.4% (w/w), and exhibited surface plasmon resonance (SPR) peaks at 420–439 nm. CHoVSB/AgNP-1 and CHoVSB/AgNP-2 composites produced were green solids with yields of 72.5 and 80.3% (w/w), and SPR peaks at 419 and 447 nm, respectively. CHoVSB/AgNP-2 composite was found the best product featuring spherical shape with a size of 21 nm and a uniform particle distribution. It has displayed the potential to be used as a food preservative with the highest percentage of bacterial reduction of 99.5 and 98.6% at a concentration of 1000 ppm for 3 and 7 days of observation, respectively.

## Keywords

chitosan, Schiff base, silver nanoparticles, antibacterial, *ortho*-vanillin

## 1 Introduction

The food industry is obligated to maintain freshness, cleanliness, and endeavor to provide the highest quality food to customers. A primary objective is the safeguarding of food against contamination by harmful microorganisms, whether they originate within or are introduced outside. Microbial contamination may compromise food, diminish its quality, and pose significant risks to human health and life [1]. Microorganisms include *Salmonella* sp., *Campylobacter* sp., *Listeria monocytogenes*, *Staphylococcus aureus*, and *Escherichia coli* often contaminate food and induce illnesses [2].

Antibacterial agents may inhibit microbial contamination of food, hence preserving food quality [3, 4]. The use of antibiotics in food is discouraged due to its adverse

effects [5]. Consequently, it is compelling to discover novel antibacterial agents that are both safe and efficacious in avoiding bacterial contamination of food. Over the last ten years, nanotechnology has developed as a pioneering invention facilitating the creation of nanometer-scale materials that may function as antimicrobials due to their extensive surface area-to-volume ratio [6].

Numerous metal nanoparticles originating from copper, zinc, gold, and silver have shown advantageous antibacterial characteristics. Silver nanoparticles (AgNPs) have the capability to suppress the proliferation of several bacterial strains [7]. The use of AgNPs as food preservatives represents a possible application within the food sector. AgNPs may effectively eliminate both gram-positive and

gram-negative bacteria, as well as fungus, while exhibiting little damage to human tissue [8]. During the synthesis of antibacterial AgNPs, a capping agent is necessary to control particle size and avoid aggregation, hence assuring the antimicrobial activity of the AgNPs [9].

A variety of materials have been investigated as capping agents for AgNPs. Chitosan is a capping agent that offers several benefits over other options [9]. Chitosan is a useful substance that has biodegradable, biocompatible, and antibacterial qualities. Numerous research has shown that chitosan serves as an effective stabilizer for AgNPs. Moreover, chitosan-AgNPs have shown considerable antibacterial and antifungal properties [10]. The efficacy of chitosan as a capping agent and subsequently as an antibacterial agent may be improved by structural modification. The active groups of chitosan, including amine ( $-\text{NH}_2$ ) and primary hydroxyl, are amenable to further modification with other groups. One of the potential modifications of chitosan is the synthesis of chitosan Schiff bases [11].

Chitosan Schiff bases include imine groups ( $>\text{C}=\text{N}-$ ) formed *via* the interaction of chitosan's amino group with aldehyde-containing substances *via* a condensation process [12]. Aldehyde-chitosan Schiff bases have been shown to prolong the shelf life of broccoli by as much as seven days [13]. Additional research indicates that aldehyde-chitosan Schiff bases have significant antibacterial efficacy against *E. coli* and *S. aureus* [14]. Heterocyclic aldehyde-chitosan Schiff bases have antifungal action against *Candida albicans* and *Candida tropicalis* [15]. *Ortho*-vanillin compounds with an aldehyde group may serve as effective capping agents. *Ortho*-vanillin Schiff bases serve as effective ligands for metals like nickel, cobalt, copper, and zinc, demonstrating significant action against *S. aureus* [16]. Vanillin has been shown as an efficient reducing agent and stabilizer in the synthesis of vanillin-AgNPs, which exhibit antibacterial action against streptococcus mutans [17]. We anticipated that the transformation of chitosan into a chitosan-*ortho*-vanillin Schiff base (CHoVSB) might be promising for the development of novel AgNPs with antibacterial and biocompatible characteristics, and minimal toxicity for use in the food sector. The production of AgNPs composites using CHoVSB as a capping agent and their use as a food preservative *via* antimicrobial testing has not been previously documented. The antibacterial efficacy of the synthesized AgNPs composites was assessed on minced chicken flesh, and following a seven-day storage period, the suppression of microbiological growth was investigated.

## 2 Experimental

### 2.1 Materials and instruments

Chitosan, characterized by a deacetylation degree of approximately 65% (as determined by Fourier transform infrared spectroscopy (FTIR)) and a molecular weight of 338 kDa (measured using a Viscometer Ubbelohde), was acquired from CV Chi-Multiguna (CV Chi-Multiguna-Indonesia). Silver nitrate, ascorbic acid, sodium hydroxide, sodium chloride, absolute ethanol, glacial acetic acid, acetone, and plate count agar were purchased from Merck, whereas *ortho*-vanillin and sodium tripolyphosphate (STTP) were sourced from Sigma Aldrich. The characterization of AgNPs was conducted using an FTIR spectrophotometer (Agilent, Cary 630 FTIR Spectrometer), an ultraviolet-visible (UV-Vis) spectrophotometer (Thermo Scientific, Genesys 10S UV-Vis), an atomic absorption spectrometer (Shimadzu AA-700), and field emission scanning electron microscopy with energy dispersive X-ray spectroscopy (FE-SEM-EDX, Jeol, JSM-6510LA).

### 2.2 Synthesis of chitosan-*ortho*-vanillin Schiff base

5 g of chitosan (0.0148 mmol) were dissolved in 250 mL 3% (v/v) aq. acetic acid solution and agitated at room temperature for 2 h until a homogenous chitosan gel was produced. 3 g of *ortho*-vanillin (19.7 mmol) was dissolved in 50 mL of 70% ethanol, and added dropwise into the chitosan solution. The reaction was halted by the gradual addition of 5% (w/v) aq. NaOH until a saturated precipitate was produced. The precipitate was filtered and rinsed with 70% ethanol till achieving a pH of 7. The chitosan-*ortho*-vanillin Schiff base (CHoVSB) residue was subjected to drying in an oven at 70 °C until a consistent mass was achieved. The product was acquired with a yield of 57.6% as a brownish-yellow solid and characterized using UV-Vis and FTIR spectroscopies.

### 2.3 Synthesis of chitosan/AgNPs and chitosan-*ortho*-vanillin Schiff base/AgNPs composites

#### 2.3.1 Procedure 1

Chitosan, or CHoVSB, at a concentration of 2% (w/v) in 100 mL of 1% (v/v) aq. acetic acid, was heated to 50 °C. 10 mL of 0.2% (w/v)  $\text{AgNO}_3$  was added dropwise to this solution, along with 10 mL of 1% (w/v) aq. ascorbic acid, and the pH was adjusted to 6. The mixture was then agitated for 1 h at 50 °C. The mixture was incrementally added to 30 mL of 1% (w/v) aq. STTP and stirred for a further 30 min. Subsequently, a 1 M aq. NaOH solution was added dropwise until the pH reached 10, followed by sonication in a water bath sonicator (42 kHz, 50 Watt, Krisbow) for

15 min. The mixture was incubated for 3 h at 60 °C, thereafter filtered, and the residue was rinsed with deionized water to achieve a pH of 7. The residue was dried in an oven at 50 °C until a consistent bulk was achieved. The corresponding residues were CH/AgNP-1 and CHoVSB/AgNP-1.

### 2.3.2 Procedure 2

Chitosan or CHoVSB at a concentration of 2% (w/v) in 100 mL of 1% (v/v) aq. acetic acid was heated to 50 °C. Subsequently, 30 mL of 1% (w/v) aq. STPP was added dropwise, and the mixture was agitated for 30 min. 10 mL of 0.2% (w/v) aq. AgNO<sub>3</sub> was added dropwise to this solution, along with 1% (w/v) aq. ascorbic acid, and the pH was adjusted to 6. The mixture was then agitated at 50 °C for 1 h. A 1 M aq. NaOH solution was added dropwise until the pH reached 10, followed by sonication in a water bath for 15 min. The mixture was incubated for 3 h at 60 °C, thereafter filtered, and the residue was rinsed with deionized water to achieve a pH of 7. The residue was subjected to drying in an oven at 50 °C until a consistent mass was achieved. The relevant residues were CH/AgNP-2 and CHoVSB/AgNP-2.

### 2.3.3 Procedure 3

CHoVSB at a concentration of 2% (w/v) in 100 mL of 1% (v/v) aq. acetic acid was heated to 50 °C. Subsequently, 30 mL of 1 g STTP in 100 mL aquademineralization (w/v) (1% STTP) was added dropwise, and the mixture was agitated for 30 min. 10 mL of 0.2% (w/v) aq. AgNO<sub>3</sub> were added dropwise to this solution, along with 10 mL of 1% ascorbic acid, and the pH was adjusted to 6. The mixture was also agitated at 50 °C for 1 h. A 1 M aq. NaOH solution was added dropwise until the pH reached 10, followed by sonication in a water bath for 15 min. Following sonication, the mixture was subjected to filtration, and the residue was rinsed with deionized water until a pH of 7 was achieved. The residue was subjected to drying in an oven at 50 °C until a consistent mass was achieved. The resultant residue was CHoVSB/AgNP-3.

### 2.3.4 Procedure 4

CHoVSB at a concentration of 2% (w/v) in 100 mL of 1% mL glacial acetic acid was agitated at ambient temperature until homogeneity was achieved. Subsequently, 30 mL of 1% STTP was added dropwise, and the mixture was agitated for 30 min. 10 mL of 0.2% (w/v) aq. AgNO<sub>3</sub> were added dropwise to this solution, along with 10 mL of 1% ascorbic acid, and the pH was adjusted to 6. The mixture was then agitated for 1 h at ambient temperature. A 1 M aq. NaOH solution was added dropwise until the pH reached 10, followed by sonication in a water bath

for 15 min. Following sonication, the mixture was subjected to filtration, and the residue was rinsed with deionized water to achieve a pH of 7. The residue was subjected to drying in an oven at 50 °C until a consistent mass was achieved. The resultant residue was CHoVSB/AgNP-4.

## 2.4 Characterization of the AgNPs composites

The interaction between AgNPs, chitosan, and CHoVSB was examined using IR spectroscopy. UV-Vis spectrophotometry was used to identify the creation of AgNPs, as shown by surface plasmon resonance (SPR) peaks. The overall silver concentration in the composites was quantified by an atomic absorption spectrometry (AAS). The shape, distribution, and dimensions of AgNPs were evaluated using FE-SEM-EDX. FE-SEM-EDX images effectively illustrate the surface features and particle size distribution, provide configuration and composition of nanoparticles. In addition, the ImageJ® software [18] is used to measure particle measuring. The average particle size and AgNPs distribution are determined by the analysis of Gaussian distribution with Origin® software [19].

## 2.5 Antibacterial activity

The antibacterial efficacy of CH/AgNP and CHoVSB/AgNP composites was determined using the procedure described by [20]. Composite sample solutions with a concentration of 2,500 ppm in 1% acetic acid were created. The positive control used was a 300-ppm ciprofloxacin solution, whereas the negative control was a 1% acetic acid solution. Minced chicken flesh (2,225 g) was sterilized by immersion in to a 0.001% sodium hypochlorite solution for 2 min. The minced chicken was encased in polyethylene and maintained at 4 °C for 7 days. Bacterial colonies were observed on days 0, 3, and 7 using the total plate count technique.

Subsequently, 10 g minced chicken was completely homogenized with 90 mL of sterile 0.9% NaCl solution to create the first dilution. Subsequent dilutions were prepared from 10<sup>-1</sup> to 10<sup>-6</sup>. 1 mL of each diluted solution was transferred onto a sterile Petri dish containing plate count agar medium. Petri plates were incubated for 24 h at ambient temperature. The bacterial colonies in each petri dish were counted visually, according to the criteria of 25–250 colonies per dish.

## 3 Result and discussion

### 3.1 Synthesis of chitosan-ortho-vanillin Schiff base

CHoVSB was synthesized by a condensation process between the main amino group of chitosan and the carbonyl group of *ortho*-vanillin (Fig. 1). The amino group of chitosan functions as a nucleophile, whereas the carbonyl group of

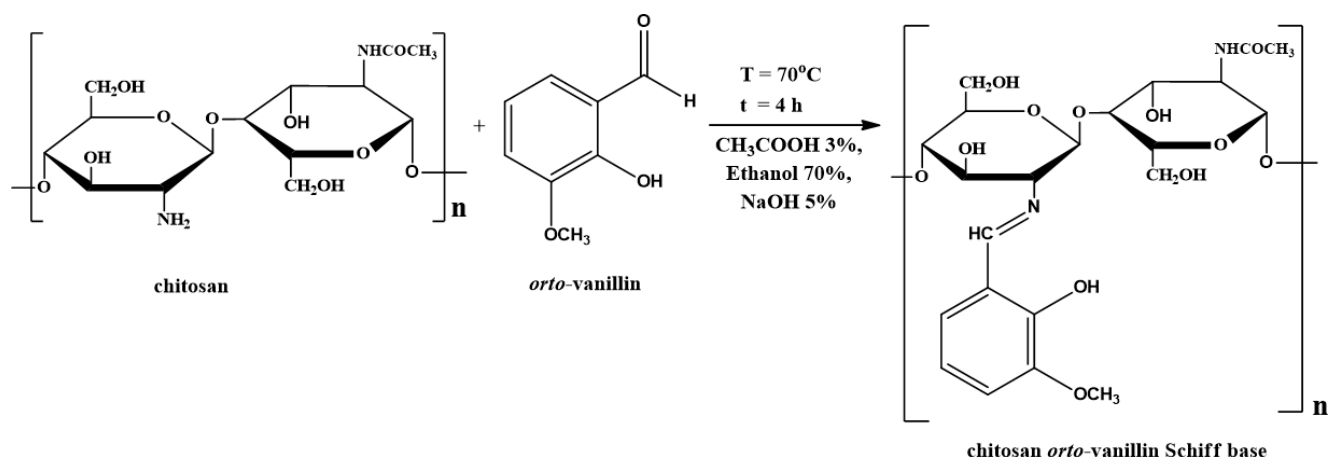


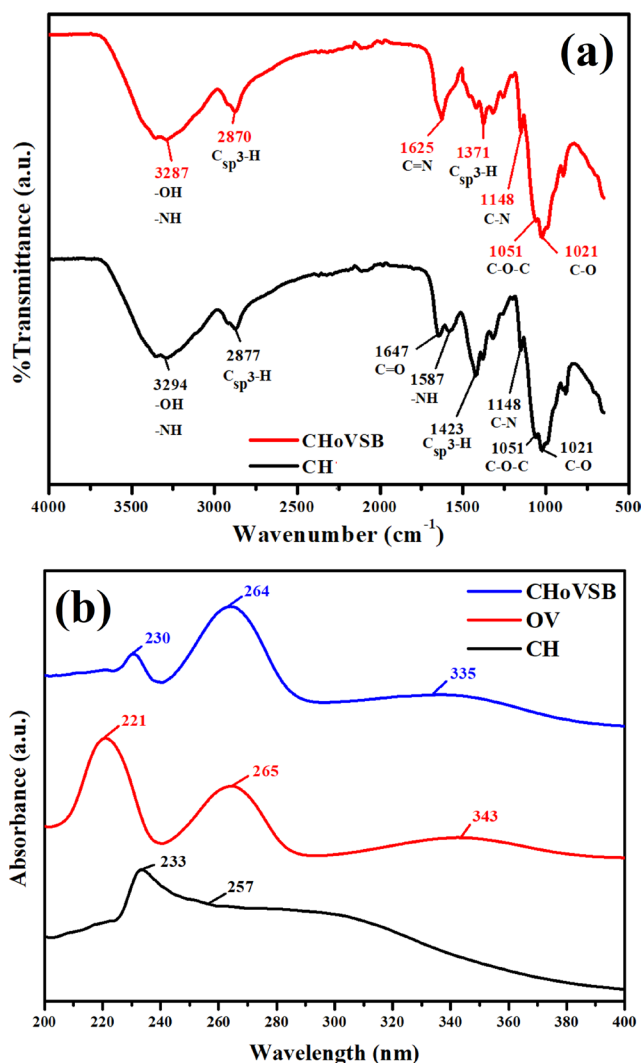
Fig. 1 General reaction of CHoVSB

*ortho*-vanillin serves as an electrophile [21]. The CHoVSB product obtained was a brownish-yellow solid with a yield of 57.6% (w/w) and a degree of substitution of 44.09%.

The effective synthesis of CHoVSB was shown by the formation of an azomethine group ( $\text{R}_1\text{HC}=\text{N}-\text{R}_2$ ). The azomethine group in CHoVSB was confirmed by the peak at  $\bar{\nu}$  1625  $\text{cm}^{-1}$  (Fig. 2(a)) [22]. The FTIR study indicates an absorption band for the  $-\text{OH}$  and  $-\text{NH}$  groups in chitosan at  $\bar{\nu}$  3294  $\text{cm}^{-1}$ , which moved to 3287  $\text{cm}^{-1}$  in CHoVSB. In chitosan, a distinct absorption was seen from the carbonyl group at 1647  $\text{cm}^{-1}$ , while an absorption at 1625  $\text{cm}^{-1}$  in the FTIR spectrum of CHoVSB was attributed to the stretching of the imine group [23]. The transition from 1647  $\text{cm}^{-1}$  to 1625  $\text{cm}^{-1}$  may be ascribed to the influence of electronegativity. In comparison to chitosan, the UV-Vis spectra of CHoVSB exhibits a novel absorption band at a wavelength of 264 nm, indicative of a  $\pi \rightarrow \pi^*$  transition of the imine group (Fig. 2(b)). The maximum value of CHoVSB was equivalent to that of *ortho*-vanillin. The application of 70% ethanol to CHoVSB will entirely eliminate the remaining *ortho*-vanillin from the CHoVSB product [24]. The peak resulted from the creation of a new imine group in CHoVSB *via* the condensation reaction between chitosan and *ortho*-vanillin.

### 3.2 Synthesis of CH/AgNP and CHoVSB/AgNP

AgNPs composites were formed by the reaction of chitosan or CHoVSB with  $\text{AgNO}_3$ , ascorbic acid, and STPP (Fig. 3, Table 1). Chitosan and CHoVSB functioned as capping agents for AgNPs, inhibiting aggregation, whereas the synthesis of AgNPs was effectively accomplished by the cross-linking of chitosan or CHoVSB with STPP. The synthesized AgNPs exhibited a reduced size range (1–100 nm) and a homogeneous size distribution [25]. The synthesis of

Fig. 2 (a) Spectra FTIR of chitosan (CH) and CHoVSB, (b) UV-Vis spectra of chitosan (CH), CHoVSB, and *ortho*-vanillin (oV)

AgNPs composites using chitosan and its derivatives demonstrates superior characteristics for surface area, dimensions, morphology, size distribution, and stability [26]. AgNPs

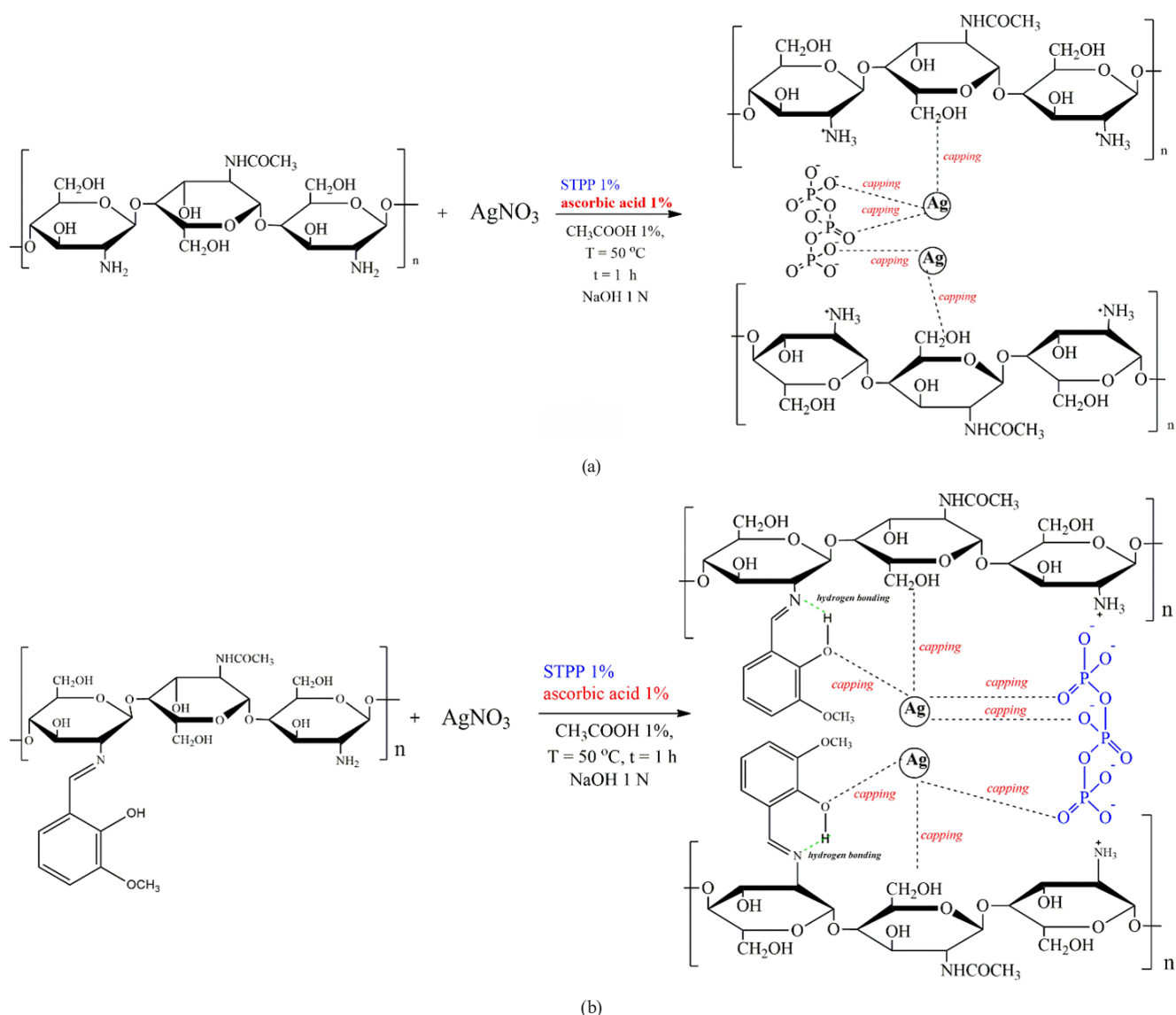


**Fig. 3** General reaction for (a) the synthesis of CH/AgNP composite, and (b) CHoVSB/AgNP composite

**Table 1** Properties of synthesized AgNPs composites

Procedure	Sample	Yield % (w/w)	SPR effect (nm)	Molar extinction coefficient ( $\epsilon$ ) (cm <sup>2</sup> /g)	Peak profile	Average size of particles (nm)	Incoming Ag adsorption by AAS (%)
1	CH/AgNP-1	83.4	420	664	Weak	99	2.86
2	CH/AgNP-2	80.8	439	598	Sharp	32	1.91
1	CHoVSB/AgNP-1	72.5	419	216	Weak	Not measured	Not measured
2	CHoVSB/AgNP-2	83.9	447	231	Sharp	21	1.63
3	CHoVSB/AgNP-3	77.9	413	183	Weak	29	1.52
4	CHoVSB/AgNP-4	87.3	425	300	Sharp	Not measured	Not measured

have significant antibacterial efficacy and has the potential to serve as broad-spectrum, stable bactericides with little toxicity [27, 28]. Moreover, a reduced size coupled with an increased surface area in AgNPs aids in preventing aggregation, hence boosting their antibacterial efficacy [27].

### 3.3 Characterization of AgNPs composites

Table 1 delineates the differences in characteristics of the produced composites. A spherical shaped AgNPs has an SPR peak at around 410 nm. These results are in line with the research that has been done previously by [29, 30]. Fig. 4 illustrates the SPR patterns of CH/AgNP and CHoVSB/

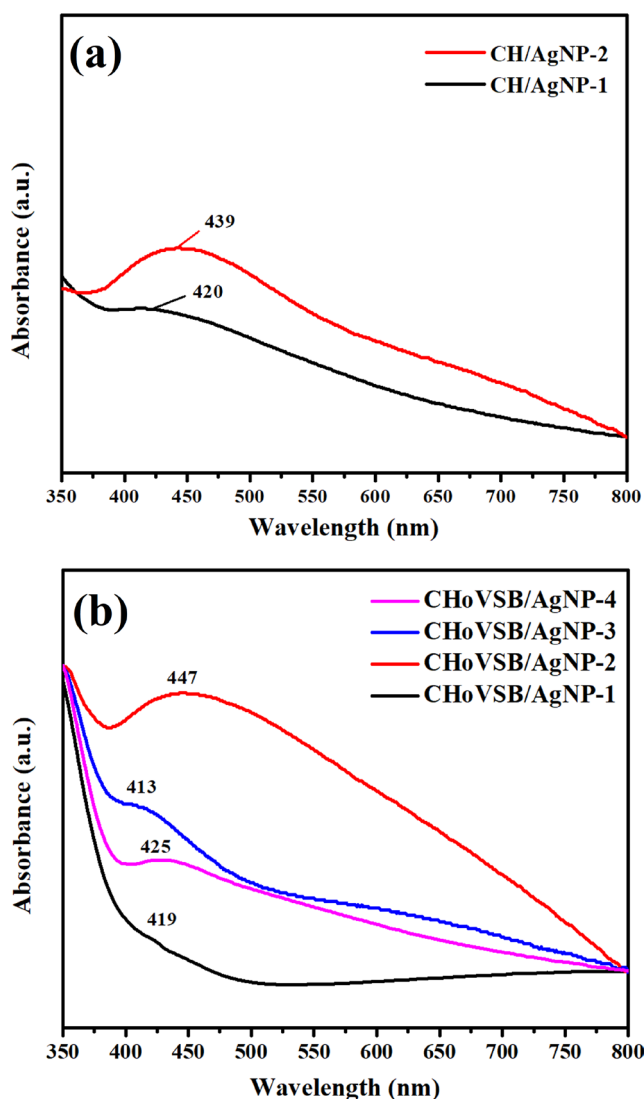


Fig. 4 UV-Vis spectra of (a) CH/AgNP composites, and (b) CHoVSB/AgNP composites

AgNPs composites. In comparison, CH/AgNP-2 (Fig. 4(a)) and CHoVSB/AgNP-2 (Fig. 4(b)) exhibit a SPR pattern characterized by a higher wavelength and robust intensity. A broader absorption peak and an increased maximum wavelength ( $\lambda_{\max}$ ) indicate a larger nanoparticle size with more vigorous oscillation [31, 32]. A symmetrical SPR peak pattern indicates homogeneous dispersion of nanoparticles [29]. The findings show that the development of cross-links between chitosan or CHoVSB and STPP prior to the reduction of  $\text{Ag}^+$  ions enhance the absorption of metal ions. The cross-linking of chitosan or CHoVSB with STPP resulted in a uniform and accessible pore structure while decreasing the degree of crystallinity [33]. Significantly, increasing the reaction temperature during the synthesis of AgNPs composites enhanced the intensity of the SPR profile [34]. Heating may facilitate molecular collisions, therefore

inhibiting the generation of undesirable side products [35]. A notable  $\lambda_{\max}$  shift in CH/AgNP-2 and CHoVSB/AgNP-2, in comparison to the corresponding AgNPs, clearly demonstrates that the second method used for synthesizing AgNPs using chitosan or CHoVSB as a capping agent was the most efficacious [36]. Simultaneously, incubation at 60 °C after sonication has enhanced the peak intensity and  $\lambda_{\max}$  values (procedures 1 and 2) [33, 34]. Consequently, CHoVSB/AgNP-2 demonstrated a superior SPR pattern compared to AgNPs (CHoVSB/AgNP-3 and CHoVSB/AgNP-4), which were not subjected to incubation after sonication. CH/AgNP-1 and -2, together with CHoVSB/AgNP-2 and -3, were used for further analysis.

Fig. 5 illustrates the FTIR spectrum of the AgNPs composites, indicating a shift and heightened absorption intensity in the O–H and N–H stretches, as well as the C=N stretch, in comparison to pure chitosan and CHoVSB. Amine (–NH) and hydroxyl groups have a strong affinity

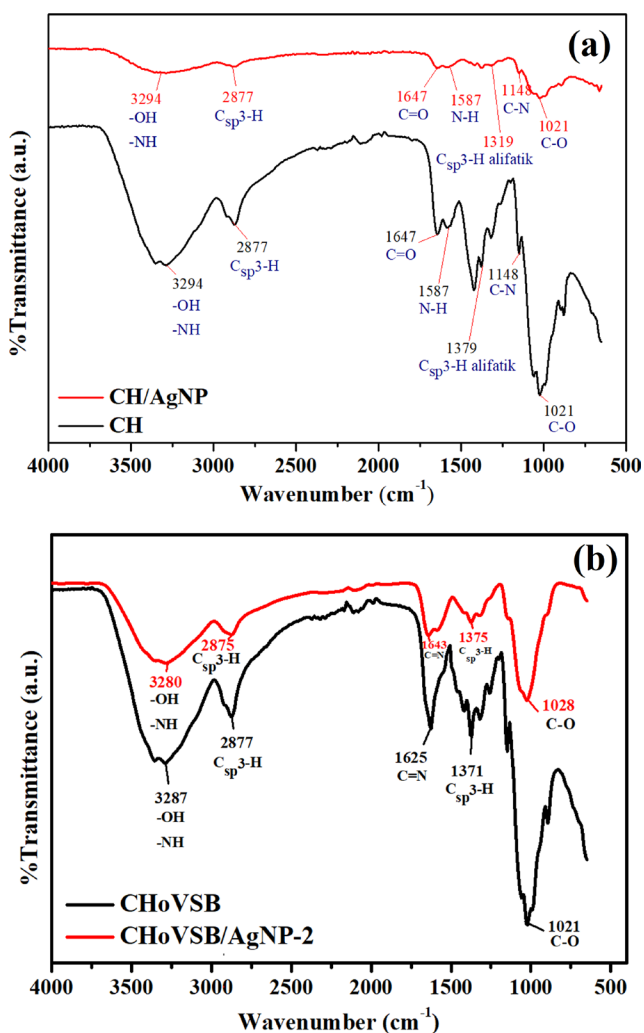


Fig. 5 FTIR spectra of (a) chitosan and CH/AgNP-2 composite, and (b) CHoVSB and CHoVSB/AgNP-2 composite

for silver ions. The disparity in electronegativity between nitrogen and oxygen atoms influences the attachment of free electrons to silver metal [37, 38]. The reduction in peak intensity for the  $>C=N-$  group, seen at around  $1640\text{ cm}^{-1}$  in CH/AgNP-2 (Fig. 5(a)) and  $1625\text{ cm}^{-1}$  in CHoVSB/AgNP-2 (Fig. 5(b)), shows that chitosan and CHoVSB effectively functioned as capping agents during the synthesis of AgNPs [11].

In CH/AgNP, the surface exhibits larger and more irregular aggregates with relatively porous characteristics, indicating a high surface area (Fig. 6(a)). The size distribution graph in Fig. 6(c) supports this observation, as the particles exhibit a broad distribution, predominantly below 30 nm, but with larger aggregates contributing to the overall average size of 99 nm. Such a structure might favor applications requiring extensive surface

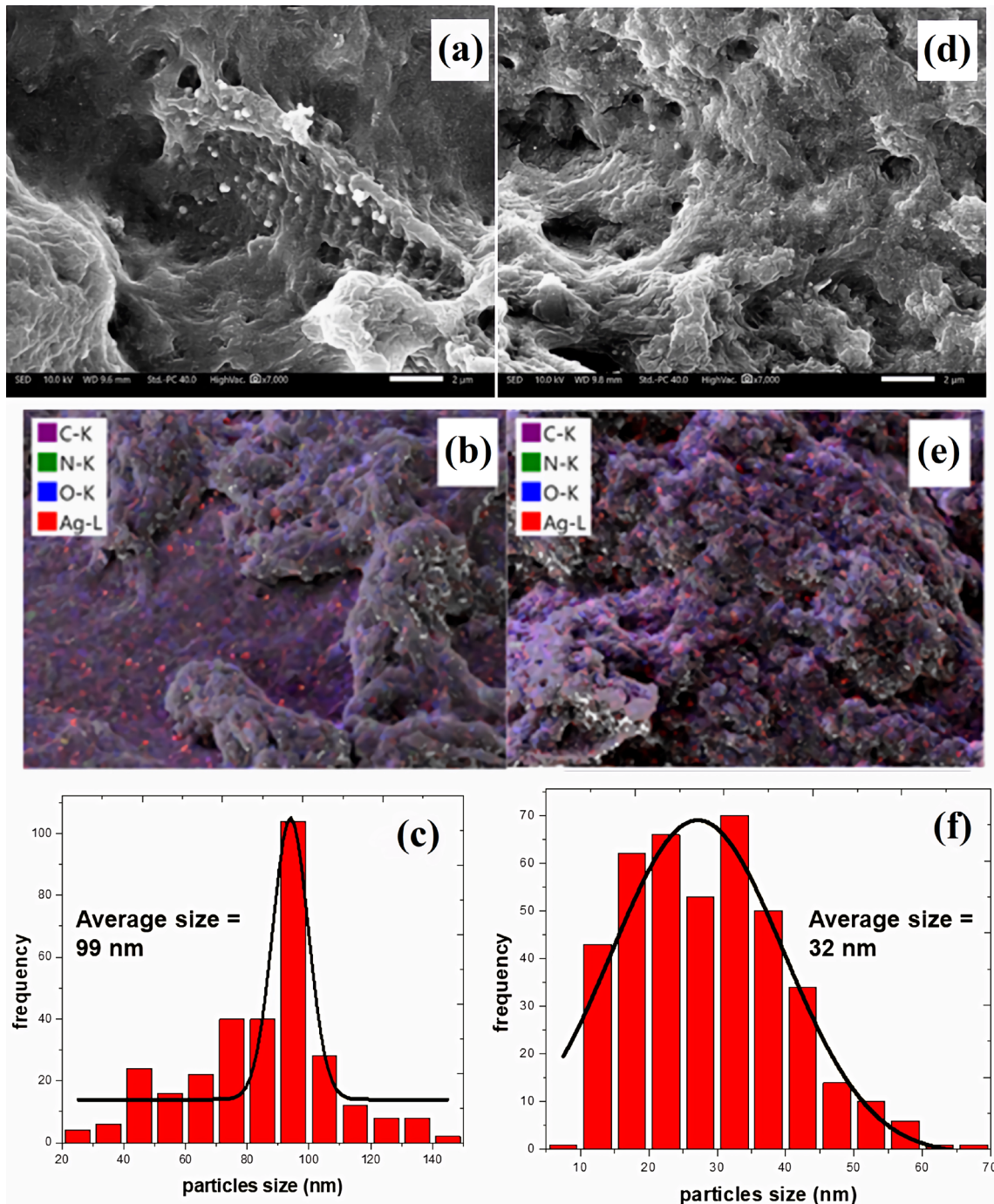


Fig. 6 CH/AgNP-1: (a) morphology, SEM image 7.000×, (b) EDX mapping, and (c) size distribution histogram; and CH/AgNP-2: (d) morphology, SEM image 7.000×, (e) EDX mapping, and (f) size distribution histogram

interaction, such as catalysis or adsorption, albeit with potential stability challenges due to the heterogeneous size distribution. Conversely, in Fig. 6(d), the surface is more uniform and compact, with smaller and more evenly distributed particles. The corresponding size distribution in Fig. 6(f) confirms this, with a tighter distribution around a significantly smaller average particle size of 32 nm. This reduced particle size, combined with the uniform morphology, suggests enhanced stability and potential for higher reactivity due to the increased surface-to-volume ratio. Moreover, elemental mapping in Fig. 6(b) and (e) highlights the uniformity of carbon, nitrogen, oxygen, and silver distributions, which is crucial for applications like electrochemical devices or antimicrobial coatings. Notably, the uniform incorporation of Ag in Fig. 6(e) may enhance functionalities such as electrical conductivity or biocidal activity. Fig. 6 shows SEM images of CH/AgNP, illustrating that AgNPs are adhered to chitosan and have a spherical morphology. CH/AgNP-2 exhibited a more uniform distribution of AgNPs and a lower average particle size of 32 nm, in contrast to CH/AgNP-1, which had an average size of 99 nm. This work has shown the impact of including STPP prior to the reduction of silver ions. The inclusion of a crosslinker enhances the stability of chitosan molecules for the adsorption of metal ions, including  $\text{Ag}^+$  ions [39]. This aligns with the EDX study, which indicated that the mass percentage of Ag in CH/AgNP-2 (1.00%) exceeded that of CH/AgNP-1 (0.26%).

The CHoVSB/AgNP-2 sample in Fig. 7(a) exhibits a dense surface with small, well-distributed nanoparticles embedded within the matrix, as reflected by the tighter particle size distribution with the smallest average size of 21 nm (Fig. 7(c)). This morphology indicates a large surface area and higher uniformity, enhancing the material's reactivity and stability. The elemental mapping in Fig. 7(b) demonstrates a homogeneous distribution of Ag alongside other elements, supporting uniform functional performance, particularly in applications like catalysis or antimicrobial coatings, where consistent nanoparticle dispersion is crucial. SEM-EDX studies confirmed that the CHoVSB/AgNP-2 composite exhibited a reduced size (21 nm) and a more uniform distribution compared to CHoVSB/AgNP-3 (28 nm) and CH/AgNP composites. The incorporation of STPP into CHoVSB prior to  $\text{Ag}^+$  ion reduction influenced the size and distribution of the AgNPs, similar to chitosan. The SEM examination indicated that the concentration and homogeneity of AgNPs on the surface of CHoVSB exceeded those of chitosan. The incorporation of hydroxyl groups in CHoVSB enhanced its capacity

to interact with AgNPs. The homogeneous distribution of AgNPs in CHoVSB/AgNP-2 was confirmed by the SPR pattern. Moreover, sonication and heating in a water bath at 50 °C significantly influenced the dimensions of the resultant nanoparticles, with sonication disrupting the aggregation of AgNPs, leading to a significant reduction and narrowing of the particle diameter. In contrast, the CHoVSB/AgNP-3 sample in Fig. 7(d) shows a slightly rougher texture with less densely packed nanoparticles compared to CHoVSB/AgNP-2. The particle size distribution in Fig. 7(f) is relatively broader, with a larger average size of 28 nm, indicating a slight compromise in surface area and uniformity. Despite this, the elemental mapping in Fig. 7(e) suggests a consistent integration of Ag and other elements, ensuring adequate functional properties and stability. EDX analysis indicated that the concentration of Ag in CHoVSB/AgNP-2 (12.77%) exceeded that in CHoVSB/AgNP-3 (5.21%), indicating superior adsorption of Ag with CHoVSB compared to chitosan. Consequently, CHoVSB is determined to be a more appropriate capping agent for the production of AgNPs compared to chitosan.

The comparison between CH/AgNP and CHoVSB/AgNP reveals distinct differences in surface morphology, particle size distribution, elemental homogeneity, and overall stability. CH/AgNP generally displays a more irregular surface with larger aggregates and broader particle size distributions, indicating higher surface area but reduced uniformity, which may impact performance consistency. In contrast, CHoVSB/AgNP exhibits a denser and more compact morphology with finer, more uniformly distributed nanoparticles, ensuring enhanced structural integrity and stability. Elemental mapping of CHoVSB/AgNP also shows superior homogeneity in silver distribution, which is crucial for consistent functional performance. While CH/AgNP may be better suited for applications emphasizing surface interactions, such as adsorption or catalysis, CHoVSB/AgNP is more advantageous for precision applications requiring stability, uniformity, and refined particle characteristics, such as antimicrobial coatings, drug delivery, or high-performance catalysts. Overall, CHoVSB/AgNP demonstrates superior material properties tailored for advanced and reliable applications.

### 3.4 Antimicrobial activity

The food preservation efficacy of the synthesized AgNPs composites was assessed using the total plate count technique on agar plate count medium, and their capability to suppress bacterial growth was tested. Fig. 8 illustrates that CHoVSB/AgNP-2 emerged as the most effective composite

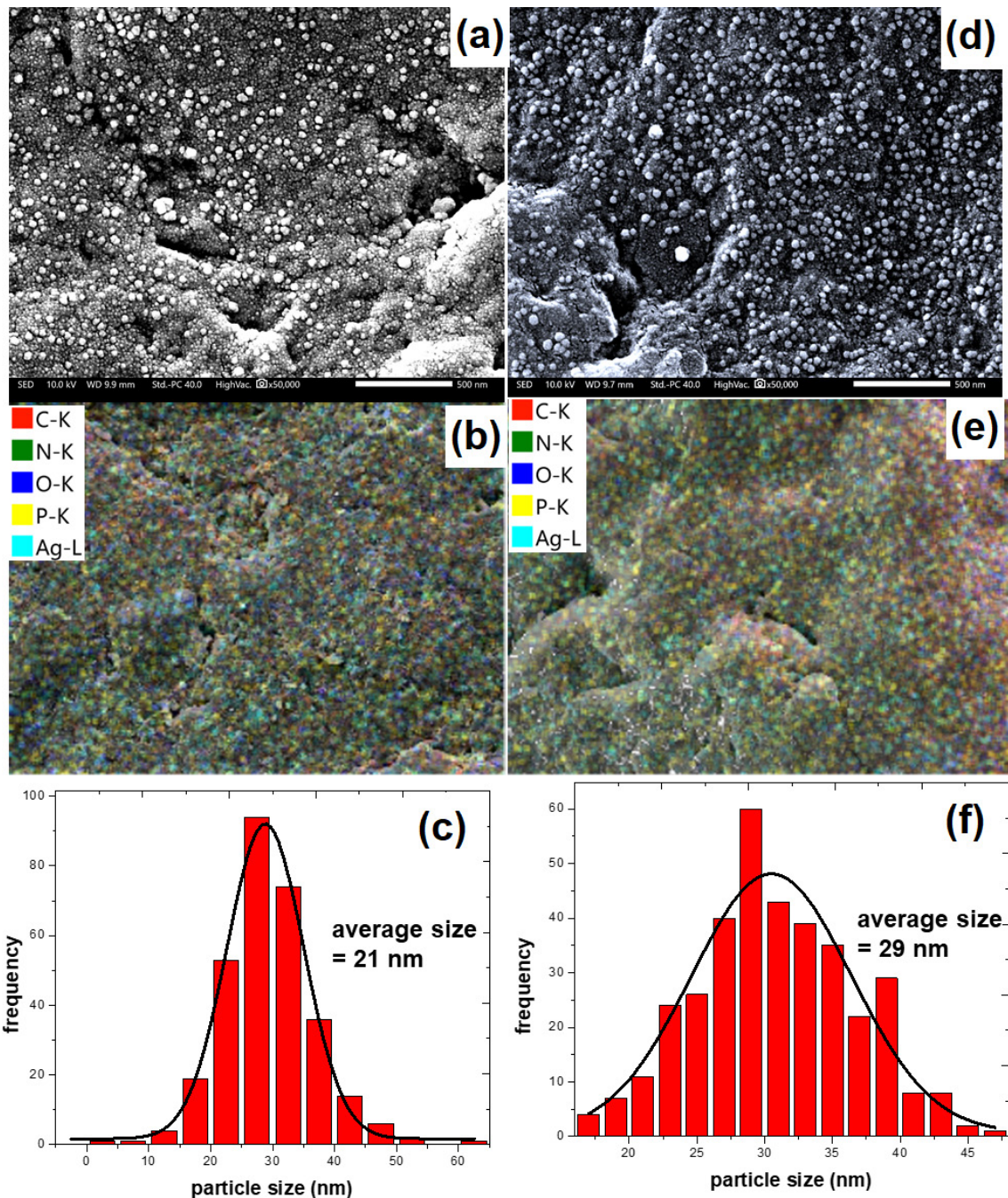


Fig. 7 CHoVSB/AgNP-2: (a) morphology, SEM image 50.000×, (b) EDX mapping, and (c) size distribution histogram; and CHoVSB/AgNP-3: (d) morphology, SEM image 50.000×, (e) EDX mapping, and (f) size distribution histogram

for suppressing bacterial growth in minced chicken flesh, with inhibition percentages of 99.5% and 98.6% on the third and seventh days, respectively [34]. The synthesized AgNPs exhibit superior antibacterial activity compared to chitosan and the Schiff base (CHoVSB) in extending the shelf life of chicken flesh by inhibiting breakdown or spoilage. The dimensions and distribution of particle size affect the antibacterial efficacy of AgNPs by modifying the surface area available for microbial interaction with minced chicken [40].

Khan et al. [41] showed that the application of a 1.5% chitosan/AgNPs composite effectively preserved rabbit meat for 16 days at 4 °C. Prior research has shown that immersing beef in a 10% AgNPs solution for 4 h may maintain the quality of the meat for a minimum of seven days [42]. Researchers have shown that chitosan and its derivatives exhibit antibacterial properties by suppressing the proliferation of pathogenic and food spoilage bacteria [43]. The polycationic groups  $\text{NH}_3^+$  or  $>\text{C}=\text{NH}^+$  interact with the anion of lipopolysaccharides on bacterial cell

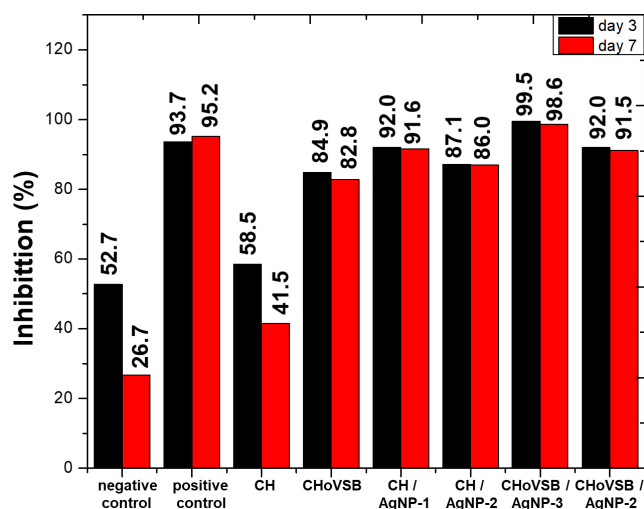


Fig. 8 Percentage decrease in the number of bacteria in the sample

membranes, interrupting activities and inducing osmotic stress owing to electrolyte leakage between cells, ultimately resulting in cell death [43]. AgNPs may also neutralize reactive oxygen species, leading to oxidative stress and impairing all bacterial functions, including protein synthesis, DNA activity, and enzyme activity.

#### 4 Conclusions

We have reported an environmentally friendly method to synthesize AgNPs composites with chitosan and CHoVSB using ascorbic acid as a bioreductant. CHoVSB was suc-

cessfully synthesized from chitosan and *ortho*-vanillin as a brownish-yellow solid with 57.6% yield and a degree of substitution of 44.09%. The efficacy of chitosan as a capping agent in the synthesis of AgNPs was functionally improved by introducing CHoVSB. The obtained data have indicated that AgNPs synthesized with CHoVSB possess a uniform particle distribution and smaller size compared to those synthesized with chitosan. The particle size of CHoVSB-AgNP is 21–29 nm while CH-AgNP are 32–99 nm. The addition of STPP before Ag<sup>+</sup> ion reduction was considered as the ideal time for synthesizing AgNPs composites with chitosan or the modified chitosan. CHoVSB/AgNP-2 was the best among other synthesized AgNPs composites that characterized by uniformly distributed spherical particles with an average size of 21 nm. It was able to inhibit the bacterial growth in the minced chicken meat stored at 4 °C. In conclusion, the CHoVSB/AgNP composite has displayed the potentiality to be used as an environmentally friendly food preservative.

#### Acknowledgement

This project is fully supported by "Sumber Dana Selain APBN UNDIP Tahun 2023-RISSET PUBLIKASI INTERNASIONAL", with assignment letter No. 569-109/UN7.D2/PP/V/2023.

#### References

- [1] Du, C., Li, S., Fan, Y., Lu, Y., Sheng, J., Song, Y. "Preparation of gelatin-chitosan bilayer film loaded citral nanoemulsion as pH and enzyme stimuli-responsive antibacterial material for food packaging", *International Journal of Biological Macromolecules*, 254, 127620, 2024.  
<https://doi.org/10.1016/j.ijbiomac.2023.127620>
- [2] Abebe, E., Gugsu, G., Ahmed, M. "Review on Major Food-Borne Zoonotic Bacterial Pathogens", *Journal of Tropical Medicine*, 2020(1), 4674235, 2020.  
<https://doi.org/10.1155/2020/4674235>
- [3] Duda-Chodak, A., Tarko, T., Petka-Poniatowska, K. "Antimicrobial Compounds in Food Packaging", *International Journal of Molecular Sciences*, 24(3), 2457, 2023.  
<https://doi.org/10.3390/ijms24032457>
- [4] Pinto, L., Tapia-Rodríguez, M. R., Baruzzi, F., Ayala-Zavala, J. F. "Plant Antimicrobials for Food Quality and Safety: Recent Views and Future Challenges", *Foods*, 12(12), 2315, 2023.  
<https://doi.org/10.3390/foods12122315>
- [5] Bacanlı, M. G. "The two faces of antibiotics: an overview of the effects of antibiotic residues in foodstuffs", *Archive of Toxicology*, 98(6), pp. 1717–1725, 2024.  
<https://doi.org/10.1007/s00204-024-03760-z>
- [6] Anjum, S., Ishaque, S., Fatima, H., Farooq, W., Hano, C., Abbasi, B. H., Anjum, I. "Emerging Applications of Nanotechnology in Healthcare Systems: Grand Challenges and Perspectives", *Pharmaceuticals*, 14(8), 707, 2021.  
<https://doi.org/10.3390/ph14080707>
- [7] Sánchez-López, E., Gomes, D., Esteruelas, G., Bonilla, L., Lopez-Machado, A. L., Galindo, R., Cano, A., ..., Souto, E. B. "Metal-Based Nanoparticles as Antimicrobial Agents: An Overview", *Nanomaterials*, 10(2), 292, 2020.  
<https://doi.org/10.3390/nano10020292>
- [8] Bruna, T., Maldonado-Bravo, F., Jara, P., Caro, N. "Silver Nanoparticles and Their Antibacterial Applications", *International Journal of Molecular Sciences*, 22(13), 7202, 2021.  
<https://doi.org/10.3390/ijms22137202>
- [9] Restrepo, C. V., Villa, C. C. "Synthesis of silver nanoparticles, influence of capping agents, and dependence on size and shape: A review", *Environmental Nanotechnology, Monitoring & Management*, 15, 100428, 2021.  
<https://doi.org/10.1016/j.enmm.2021.100428>

- [10] Zaitun Hasibuan, P. A., Yuandani, Tanjung, M., Gea, S., Pasaribu, K. M., Harahap, M., Perangin-Angin, Y. A., Prayoga, A., Ginting, J. G. "Antimicrobial and antihemolytic properties of a CNF/AgNP-chitosan film: A potential wound dressing material", *Heliyon*, 7(10), e08197, 2021.  
<https://doi.org/10.1016/j.heliyon.2021.e08197>
- [11] Alharthi, S. S., Gomathi, T., Joseph, J. J., Rakshavi, J., Florence, J. A. K., Sudha, P. N., Rajakumar, G., Thiruvengadam, M. "Biological activities of chitosan-salicylaldehyde schiff base assisted silver nanoparticles", *Journal of King Saud University - Science*, 34(6), 102177, 2022.  
<https://doi.org/10.1016/j.jksus.2022.102177>
- [12] Rachmawati, I. E., Ngadiwiyana, Ismiyarto "Sintesis turunan azomethin sebagai zat aktif inhibitor korosi pada logam menggunakan bahan dasar piperonal dan 2-aminopiridin" (Synthesis of azomethine derivatives as active substances of corrosion inhibitors on metals using piperonal and 2-aminopyridine base materials), *Jurnal Kimia Sains dan Aplikasi*, 20(3), pp. 136–139, 2017. (in Indonesian) [online] Available at: <https://ejournal.undip.ac.id/index.php/ksa/article/view/16752/12183> [Accessed: 31 July 2024]
- [13] Lin, J., Meng, H., Guo, X., Tang, Z., Yu, S. "Natural Aldehyde-Chitosan Schiff Base: Fabrication, pH-Responsive Properties, and Vegetable Preservation", *Foods*, 12(15), 2921, 2023.  
<https://doi.org/10.3390/foods12152921>
- [14] Omer, A. M., Eltaweil, A. S., El-Fakharany, E. M., Abd El-Monaem, E. M., Ismail, M. M. F., Mohy-Eldin, M. S., Ayoup, M. S. "Novel Cytocompatible Chitosan Schiff Base Derivative as a Potent Antibacterial, Antidiabetic, and Anticancer Agent", *Arabian Journal for Science and Engineering*, 48(6), pp. 7587–7601, 2023.  
<https://doi.org/10.1007/s13369-022-07588-6>
- [15] Ali, M., Sholkamy, E. N., Alobaidi, A. S., Al-Muhanna, M. K., Barakat, A. "Synthesis of Schiff Bases Based on Chitosan and Heterocyclic Moiety: Evaluation of Antimicrobial Activity", *ACS Omega*, 8(49), pp. 47304–47312, 2023.  
<https://doi.org/10.1021/acsomega.3c08446>
- [16] Gurusamy, S., Sankarganesh, M., Revathi, N., Asha, R. N., Mathavan, A. "Synthesis and structural investigation of o-Vanillin scaffold Schiff base metal complexes: Biomolecular interaction and molecular docking studies", *Journal of Molecular Liquids*, 369, 120941, 2023.  
<https://doi.org/10.1016/j.molliq.2022.120941>
- [17] Anishya, D., Jain, R. K. "Vanillin-Mediated Green-Synthesised Silver Nanoparticles' Characterisation and Antimicrobial Activity: An In-Vitro Study", *Cureus*, 16(1), e51659, 2024.  
<https://doi.org/10.7759/cureus.51659>
- [18] National Institutes of Health "ImageJ®", [computer program] Available at: <https://imagej.net/ij/download.html> [Accessed: 22 June 2024]
- [19] OriginLab Corporation "OriginPro®, (version 8.5)", [computer program] Available at: <https://www.originlab.com/index.aspx?go=Products/Origin> [Accessed: 10 October 2023]
- [20] Badawy, M. E. I., Lotfy, T. M. R., Shawir, S. M. S. "Preparation and antibacterial activity of chitosan-silver nanoparticles for application in preservation of minced meat", *Bulletin of the National Research Centre*, 43(1), 83, 2019.  
<https://doi.org/10.1186/s42269-019-0124-8>
- [21] Ismiyarto, Handayani, W. S., Ngadiwiyana, Sarjono, P. R., Prasetya, N. B. A. "Synthesis of chitosan-salicylaldehyde/vanillin Schiff base as antibacterial active compound on cotton fabrics", *Journal of Physics: Conference Series*, 1943, 012164, 2020.  
<https://doi.org/10.1088/1742-6596/1943/1/012164>
- [22] Manju, S., Kannan, R., Kumar, V., Sudha, P. N. "Synthesis, characterization and applications of chitosan-o-vanillin schiff bases/polypropylene glycol blend", In: *National Conference on Emerging Trends and Future Challenges in Chemical Sciences P.G & Research Department of Chemistry, Shanmuga Industries Arts and Science College, Tiruvannamalai, India, 2017*, pp. 32–42.
- [23] Huang, C., Liao, H., Ma, X., Xiao, M., Liu, X., Gong, S., Shu, X., Zhou, X. "Adsorption performance of chitosan Schiff base towards anionic dyes: Electrostatic interaction effects", *Chemical Physics Letters*, 780, 138958, 2021.  
<https://doi.org/10.1016/j.cplett.2021.138958>
- [24] Mao, H., Chen, H., Jin, M., Wang, C., Xiao, Z., Niu, Y. "Measurement and correlation of solubility of o-vanillin in different pure and binary solvents at temperatures from 273.15 K to 303.15 K", *The Journal of Chemical Thermodynamics*, 150, 106199, 2020.  
<https://doi.org/10.1016/j.jct.2020.106199>
- [25] Hasan, K. M. F., Xiaoyi, L., Shaoqin, Z., Horváth, P. G., Bak, M., Bejő, L., Sipos, G., Alpár, T. "Functional silver nanoparticles synthesis from sustainable point of view: 2000 to 2023 – A review on game changing materials", *Heliyon*, 8(12), e12322, 2022.  
<https://doi.org/10.1016/j.heliyon.2022.e12322>
- [26] Joudeh, N., Linke, D. "Nanoparticle classification, physicochemical properties, characterization, and applications: a comprehensive review for biologists", *Journal of Nanobiotechnology*, 20(1), 262, 2022.  
<https://doi.org/10.1186/s12951-022-01477-8>
- [27] Lasera, A. G., Aritonang, H. F., Koleangan, D. H. "Sintesis dan karakterisasi nanopartikel CuFe<sub>2</sub>O<sub>4</sub> serta aplikasinya sebagai antibakteri" (Synthesis and characterization of nanoparticles CuFe<sub>2</sub>O<sub>4</sub> and applications as antibacterial), *Chemistry Progress*, 12(2), pp. 88–92, 2019. (in Indonesian)  
<https://doi.org/10.35799/cp.12.2.2019.27312>
- [28] Dove, A. S., Dzurny, D. I., Dees, W. R., Qin, N., Nunez Rodriguez, C. C., Alt, L. A., Ellward, G. L., Best, J. A., Rudawski, N. G., Fujii, K., Czyż, D. M. "Silver nanoparticles enhance the efficacy of aminoglycosides against antibiotic-resistant bacteria", *Frontiers in Microbiology*, 13, 1064095, 2023.  
<https://doi.org/10.3389/fmicb.2022.1064095>
- [29] Ider, M., Abderrafi, K., Eddahbi, A., Ouaskit, S., Kassiba, A. "Silver Metallic Nanoparticles with Surface Plasmon Resonance: Synthesis and Characterizations", *Journal of Cluster Science*, 28(3), pp. 1051–1069, 2017.  
<https://doi.org/10.1007/s10876-016-1080-1>
- [30] Khan, Z., AL-Thabaiti, S. A. "Chitosan capped silver nanoparticles: Adsorption and photochemical activities", *Arabian Journal of Chemistry*, 15(11), 104154, 2022.  
<https://doi.org/10.1016/j.arabjc.2022.104154>
- [31] Amirjani, A., Firouzi, F., Haghshenas, D. F. "Predicting the Size of Silver Nanoparticles from Their Optical Properties", *Plasmonics*, 15(4), pp. 1077–1082, 2020.  
<https://doi.org/10.1007/s11468-020-01121-x>

- [32] Paramelle, D., Sadovoy, A., Gorelik, S., Free, P., Hobley, J., Fernig, D. G. "A rapid method to estimate the concentration of citrate capped silver nanoparticles from UV-visible light spectra", *Analyst*, 139(19), pp. 4855–4861, 2014.  
<https://doi.org/10.1039/C4AN00978A>
- [33] Hamidi, F., Azadi Aghdam, M., Johar, F., Mehdinejad, M. H., Baghani, A. N. "Ionic gelation synthesis, characterization and adsorption studies of cross-linked chitosan-tripolyphosphate (CS-TPP) nanoparticles for removal of As (V) ions from aqueous solution: kinetic and isotherm studies", *Toxin Reviews*, 41(3), pp. 795–805, 2022.  
<https://doi.org/10.1080/15569543.2021.1933532>
- [34] Kulikouskaya, V., Hileuskaya, K., Kraskouski, A., Kozerozhets, I., Stepanova, E., Kuzminski, I., You, L., Agabekov, V. "Chitosan-capped silver nanoparticles: A comprehensive study of polymer molecular weight effect on the reaction kinetic, physicochemical properties, and synergetic antibacterial potential", *SPE Polymers*, 3(2), pp. 77–90, 2022.  
<https://doi.org/10.1002/pls2.10069>
- [35] Martha, A. A., Permatasari, D. I., Dewi, E. R., Wijaya, N. A., Kunarti, E. S., Rusdiarso, B., Nuryono, N. "Natural Magnetic Particles/Chitosan Impregnated with Silver Nanoparticles for Antibacterial Agents", *Indonesian Journal of Chemistry*, 22(3), pp. 620–629, 2022.  
<https://doi.org/10.22146/ijc.68691>
- [36] Aziz, S. B., Abdullah, O. G., Saber, D. R., Rasheed, M. A., Ahmed, H. M. "Investigation of Metallic Silver Nanoparticles through UV-Vis and Optical Micrograph Techniques", *International Journal of Electrochemical Science*, 12(1), pp. 363–373, 2017.  
<https://doi.org/10.20964/2017.01.22>
- [37] Hajji, S., Salem, R. B. S-B., Hamdi, M., Jellouli, K., Ayadi, W., Nasri, M., Boufi, S. "Nanocomposite films based on chitosan-poly(vinyl alcohol) and silver nanoparticles with high antibacterial and antioxidant activities", *Process Safety and Environmental Protection*, 111, pp. 112–121, 2017.  
<https://doi.org/10.1016/j.psep.2017.06.018>
- [38] Nate, Z., Moloto, M. J., Mubiayi, P. K., Sibiya, P. N. "Green synthesis of chitosan capped silver nanoparticles and their antimicrobial activity", *MRS Advances*, 3(42), pp. 2505–2517, 2018.  
<https://doi.org/10.1557/adv.2018.368>
- [39] Hidaka, M., Kojima, M., Sakai, S., Delattre, C. "Characterization of Chitosan Hydrogels Obtained through Phenol and Tripolyphosphate Anionic Crosslinking", *Polymers*, 16(9), 1274, 2024.  
<https://doi.org/10.3390/polym16091274>
- [40] Shehabeldine, A. M., Salem, S. S., Ali, O. M., Abd-Elsalam, K. A., Elkady, F. M., Hashem, A. H. "Multifunctional Silver Nanoparticles Based on Chitosan: Antibacterial, Antibiofilm, Antifungal, Antioxidant, and Wound-Healing Activities", *Journal of Fungi*, 8(6), 612, 2022.  
<https://doi.org/10.3390/jof8060612>
- [41] Khan, S., Hashim, S. B. H., Arslan, M., Zhang, K., Siman, L., Mukhtar, A., Zhihua, L., Tahir, H. E., Zhai, X., Shishir, M. R. I., Xiaobo, Z. "Development of an active biogenic silver nanoparticles composite film based on berry wax and chitosan for rabbit meat preservation", *International Journal of Biological Macromolecules*, 27, 133128, 2024.  
<https://doi.org/10.1016/j.ijbiomac.2024.133128>
- [42] Oluwatofarati, S. W., Olayemi, R. A., Rahman, A. "Effects of silver bio-nanoparticle treatment on the wet preservation, technological, and chemical qualities of meat", *Food Quality and Safety*, 2(3), pp. 159–164, 2018.  
<https://doi.org/10.1093/fqsafe/fyy014>
- [43] Jiang, A., Patel, R., Padhan, B., Palimkar, S., Galgali, P., Adhikari, A., Varga, I., Patel, M. "Chitosan Based Biodegradable Composite for Antibacterial Food Packaging Application", *Polymers*, 15(10), 2235, 2023.  
<https://doi.org/10.3390/polym15102235>